# On the Implementation of Blind Interference Alignment with Single-Radio Parasitic Antennas

# On the Implementation of Blind Interference Alignment with Single-Radio Parasitic Antennas

Rongrong Qian, *Student Member, IEEE*, Mathini Sellathurai, *Senior Member, IEEE*

***Abstract*—This paper studies the electronically steerable parasitic array radiator (ESPAR) antenna as a solution for beampattern switching to implement blind interference alignment (BIA) [1]. The ESPAR antenna uses a single radio-frequency (RF) chain, and its beamforming is achieved by simply tuning the reactance loads of parasitic elements. Furthermore, ESPAR's beampattern can be designed to enhance the received signal-to-noise ratio (SNR), thereby improving the performance of BIA. The focus of this work is the design of the ESPAR beampattern to realize and improve BIA. In the first approach, each receiver ESPAR antenna dynamically selects the proper beampatterns from among the sector beampatterns, which are pre-designed to access different angular sectors with constant optimal antenna efficiency. We also propose a singular value decomposition (SVD) beamforming method, by means of the available channel state information at the receiver and a dynamic matching network for a high antenna efficiency. The simulation results illustrate the improvement of BIA with proposed methods, especially in the low and moderate SNR region, due to ESPAR's beamforming capability.**

***Index Terms*—ESPAR, blind IA, beamforming.**

## I. Introduction

As a solution for spectral efficiency, multiple-user multiple-input-multiple-output (MU-MIMO) techniques have been introduced to attain more degrees of freedom (DoFs) without increasing antennas or complexity at the receiver (Rx). Generally, MU-MIMO techniques, like linear zero-forced beamforming (LZFBF), dirty-paper-coding and interference alignment, require perfect, sometimes global, knowledge of channel state information (CSI) at the transmitter (Tx) and at the Rx (referred to as CSIT and CSIR, respectively) to achieve the optimal DoFs [2]. However, in real wireless systems, acquiring CSIT is a challenging task and also leads to signaling overheads. Therefore, MU-MIMO techniques to achieve the maximum DoFs without requirements of CSIT have gained increasing interest.

Recently, a technique termed "blind interference alignment" (BIA) [1] has been developed for the MU multiple-input-single-output (MISO) broadcast channel (BC) to align inter-user interference into a reduced subspace, with no CSIT. The key to BIA is the use of a reconfigurable antenna, capable of dynamically changing its mode (e.g., frequency, polarization or beampattern) at the Rx. It has been demonstrated that, in the $K$-user $N_t \times 1$ MISO BC, BIA achieves $\frac{N_t K}{N_t+K-1}$ DoFs [1], the optimal achievable DoFs in the absence of CSIT. In [3], the performance of BIA with a cluster-based method and frequency reuse scheme has been analyzed. In [4], different code structures and the power allocation method have been studied for the design of BIA in cellular systems. However, in most of the literature, it is simply assumed that channels seen by a Rx associated with different antenna modes are independent identically distributed (i.i.d) fading channels.

Among the potential antenna mode switches, beampattern switching is an easier method to be implemented by a reconfigurable antenna system, since frequency switching requires a larger frequency band, while polarization switching may be only suitable for communication systems that are insensitive to Tx and Rx orientations. Moreover, a directional beampattern can be used to improve the received SNR by spatial filtering, thereby alleviating the impact of noise enhancement, an inherent problem of BIA. For many applications, a reconfigurable antenna with a single RF chain is more attractive, since it remarkably reduces the size, cost and power consumption of an antenna system. As mentioned above, the ESPAR antenna [5] is a good choice as the beampattern switching solution for BIA implementation. The ESPAR antenna is capable of adaptively controlling its beampattern using only a single RF chain. This functionality is achieved by exploiting mutual coupling between the closely spaced active element and parasitic elements. A small inter-element spacing in the ESPAR array leads to strong mutual coupling between elements, so that, once the signal has been excited at the RF port connected to the active element, currents are induced on all elements. Adjusting reactance loads of parasitic elements in turn changes the currents on all elements, and thus the beampattern of the array. The first attempt to apply the ESPAR antenna for BIA has been shown in our earlier work [6], [7]. However, the previous work considers the system with only $N_t = 2$ Tx antennas, and the problem of antenna efficiency is ignored.

In this work, we consider the ESPAR antenna used as a practical solution of beampattern switching to implement BIA [1], and, in particular, we investigate the beampattern design strategies for an Rx ESPAR antenna to provide $N_t$ beampatterns required by BIA. Two beamforming methods are proposed for the BIA scheme using ESPAR antennas, where antenna efficiency has been taken into account. Firstly, in the method of beampattern selection, a number of sector beampatterns with a constant optimal antenna efficiency are pre-designed, and then the Rx dynamically selects $N_t$ ones with the largest received powers. Secondly, by exploiting the available CSIR, an adaptive beamforming method based on SVD of the channel matrix obtained by the reactance domain technique is developed. SVD beamforming has been studied

R. Qian and M. Sellathurai are with the ISSS, School of Engineering & Physical Sciences, Heriot-Watt University, Edinburgh, EH14 4AS, United Kingdom. E-mail: R.Qian@hw.ac.uk, M.Sellathurai@hw.ac.uk. R. Qian is the corresponding author.)

Manuscript received XXX, XX, 2015; revised XXX, XX, 2015.

for the ESPAR to achieve the beamspace MIMO transmission [8]. In this work, the SVD beamforming is modified as a three-step strategy using the genetic algorithm to optimize reactance loads and a dynamic matching network for a high antenna efficiency. We compare the performance of BIA with the adaptive beamforming to that exploiting pre-designed directional beampatterns.

The rest of the paper is organized as follows. The system model and a brief review of BIA are given in Section II. The ESPAR beamforming methods for BIA using ESPARs are presented in Section III. The performance of the proposed schemes are evaluated in Section IV. Section V concludes the paper.

## II. System Model and BIA

### A. MU-MIMO BC with ESPAR Receivers

Consider the downlink of a $K$-user $N_t \times 1$ MISO BC. The Tx, having $N_t$ antennas, simultaneously serves $K$ users, each of which is equipped with an $(M+1)$-element ESPAR antenna. The ESPAR antenna has one active element, located at the center of a circle, and $M$ parasitic elements sit at equal angular separations on the circle, with a small inter-element spacing. The active element is fed to an RF source with an impedance, $Z_s$, while each of the parasitic elements is loaded with a tunable reactance value, $jx_m, m \in \{1, \cdots, M\}$, attained by a simple control circuit composed of a variable reactor (varactor) diode or an arrangement of varactor diodes [9]. ESPAR beamforming is achieved by tuning the reactance loads. In this system, a Rx ESPAR antenna is required to switch between $N_b$ beampatterns, where $N_b \geq N_t$. Moreover, the number of parasitic elements is also assumed to be $M \geq N_t$.

Let the vector $\hat{\boldsymbol{x}}_{n_b} = [x_1, \cdots, x_M]^T$ store the reactance values used to form the $n_b$-th beampattern, and the diagonal loading matrix is given by $\boldsymbol{X}_{n_b} = \text{diag}([Z_s, j\hat{\boldsymbol{x}}_{n_b}^T])$, where $n_b \in \{1, \cdots, N_b\}$. Thus, the $(M+1)$-dimensional equivalent weight vector for the $n_b$-th beampattern is expressed as [5]

$$\boldsymbol{w}_{n_b} = (\boldsymbol{Z} + \boldsymbol{X}_{n_b})^{-1}\boldsymbol{u}_0, \tag{1}$$

where $\boldsymbol{Z} \in \mathbb{C}^{(M+1)\times(M+1)}$ is the antenna mutual impedance matrix, which can be calculated for an array of arbitrary elements through electromagnetic modelling software. $\boldsymbol{u}_0 = [1, 0, \cdots, 0]^T \in \mathbb{Z}^{M+1}$ is a selection vector. Focusing on the 2-D propagation analysis, the $n_b$-the beampattern is

$$B_{n_b}(\theta) = \boldsymbol{w}_{n_b}^T \boldsymbol{a}_r(\theta), \tag{2}$$

where $\boldsymbol{a}_r(\theta) \in \mathbb{C}^{M+1}$ is the steering vector determined by the geometry of an ESPAR array, and $\theta$ denotes the azimuth angle. $(\cdot)^T$ is the transpose operation. The input impedance seen by the active port, $Z_{in,n_b}$, is a function of induced currents [10]:

$$Z_{in,n_b} = \boldsymbol{Z}(1,1) + \frac{1}{\boldsymbol{i}_{n_b}(1)} \sum_{m=2}^{M+1} \boldsymbol{Z}(1,m)\boldsymbol{i}_{n_b}(m), \tag{3}$$

where $\boldsymbol{X}(m,n)$ represents the $(m,n)$-th element of a matrix, and $\boldsymbol{x}(m)$ is the $m$-th element of a vector. The current vector is related to the equivalent weight vector by $\boldsymbol{i}_{n_b} = V_s \boldsymbol{w}_{n_b}$, where $V_s$ is the driving voltage in the active element. Energy losses in an ESPAR antenna system are accounted for principally by mismatch between $Z_s$ and $Z_{in,n_b}$, when the ohmic loss is negligible. Antenna efficiency of the ESPAR antenna is thus calculated as $\eta_{n_b} = 1 - |(Z_{in,n_b} - Z_s^*)/(Z_{in,n_b} + Z_s)|$, where $(\cdot)^*$ is the complex conjugate. It is noted that the input impedance is determined by the normalized currents, which in turn implies that it is a function of the reactance loads. Therefore, the reactance loads affect the antenna efficiency.

Consider the geometric channel model with $N_s$ scatterers. Each path $i$ has a single angle of departure (AoD), $\theta_{t,i}$, a single angle of arrival (AoA), $\theta_{r,i}$, and a complex gain, $\alpha_i$, followed by the i.i.d Rayleigh fading, where $i \in \{1, \cdots, N_s\}$. Without loss of generality, consider user $k$, $k \in \{1, \cdots, K\}$, whose $1 \times N_t$ channel vector related to beampattern $B_{n_b}$ can be expressed as

$$\boldsymbol{h}^{[k]}(B_{n_b}) = \sum_{i=1}^{N_s} \alpha_i B_{n_b}(\theta_{r,i})\boldsymbol{a}_t^H(\theta_{t,i}) = \boldsymbol{w}_{n_b}^T \boldsymbol{A}_r(\boldsymbol{\theta}_r)\boldsymbol{H}_a \boldsymbol{A}_t^H(\boldsymbol{\theta}_t), \tag{4}$$

where $\boldsymbol{a}_t(\theta) \in \mathbb{C}^{N_t}$ is the Tx steering vector, and the vector $\boldsymbol{\theta}_t$ stores $N_s$, and $\boldsymbol{A}_t(\boldsymbol{\theta}_t)$ is thus the matrix composed of columns of Tx steering vectors corresponding to $N_s$ AoDs. Similarly, $\boldsymbol{\theta}_r$ and $\boldsymbol{A}_r(\boldsymbol{\theta}_r)$ are AoA vector and Rx steering matrix, respectively. $\boldsymbol{H}_a$ is an $N_s \times N_s$ diagonal matrix with $\{\alpha_i\}_{i=1}^{N_s}$ as the diagonal entries. $(\cdot)^H$ is the Hermitian transpose. The signal received at user $k$ at time $t$, when its ESPAR antenna switches to $B_{n_b}$, is given by

$$y^{[k]}(t) = \sqrt{\eta_{n_b}}\boldsymbol{h}^{[k]}(B_{n_b})\boldsymbol{s}(t) + z^{[z]}(t), \tag{5}$$

where $\boldsymbol{s}(t) \in \mathbb{C}^{N_t}$ is the transmitted signal vector, and $z^{[k]} \sim \mathcal{CN}(0, \sigma_z)$ is the additive while Gaussian noise (AWGN) with zero-mean and variance $\sigma_z$. The input of the channel is subjected to the average power constraint, i.e., $\mathbb{E}\{\|\boldsymbol{s}(t)\|^2\} \leq P_t$, where $P_t$ is the total transmit power. It is noted that adjusting the reactance loads of one Rx ESPAR antenna to form different beampatterns leads to different channels seen by that Rx, where the antenna efficiency has to be taken into account. Throughout this wok, we assume that the system has no CSIT, but each Rx has perfect knowledge of the channel.

### B. BIA Based on Beampattern Switching

This subsection briefly presents the BIA approach [1] implemented by beampattern switching at the Rx. To explain how the beampattern switching can be used to align inter-user interference in BIA, we consider the simplest 2-user $2 \times 1$ MISO BC case. For the case with more $N_t$ and $K$, the detailed solutions can be found in [1].

The key to BIA is to exploit the channel correlation structures of the Rxs (termed as super-symbol), created by beampattern switching at individual Rxs. As shown in Fig. 1, the super-symbol is constructed as that Rx 1 switches its ESPAR's beampattern to $B_1$ at the first and third symbol periods and switches to $B_2$ at the second symbol period; meanwhile, Rx 2 switches to $B_1$ at the first and second symbol periods, and switches to $B_2$ at the third symbol period. These channel-correlated structures are used by the Tx jointly with a space-time coding.

It is demonstrated that BIA allows the transmitting of $N_t = 2$ symbols to each of 2 users over $N_t + K - 1 = 3$

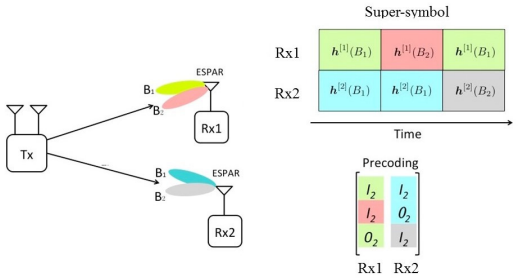


Fig. 1: Super-symbol for the 2-user $2 \times 1$ MISO BC.

symbol extensions; thus, BIA achieves $\frac{N_t K}{N_t+K-1} = \frac{4}{3}$ DoF. After interference cancellation by a simple linear combination of measurements over one super-symbol, the achievable sum-rate for a $K$-user $N_t \times 1$ MISO BC, with a constant power allocation, is given by [4]

$$C = \sum_{k=1}^{K} \frac{1}{N_t + K - 1} \mathbb{E}\left\{\log\left|\boldsymbol{I}_{N_t} + \frac{P_t}{N_t}\tilde{\boldsymbol{H}}^{[k]}\tilde{\boldsymbol{H}}^{[k]H}\right|\right\}, \quad (6)$$

where $\tilde{\boldsymbol{H}}^{[k]} \in \mathbb{C}^{N_t \times N_t}$, in which the $j$-th column vector has the form of $\tilde{\boldsymbol{H}}^{[k]}_{\cdot j} = \sqrt{\frac{\eta_j}{2K-1}}\boldsymbol{h}^{[k]T}(B_j)$ for $j = 1, \cdots, N_t - 1$ and $\tilde{\boldsymbol{H}}^{[k]}_{\cdot N_t} = \sqrt{\eta_{N_t}}\boldsymbol{h}^{[k]T}(B_{N_t})$.

## III. ESPAR Beampattern Design for BIA

This section presents the two beamforming methods for BIA using ESPARs, providing $N_t$ beampatterns to be used across one super-symbol. It is noted that, since beamforming is independently operated at each Rx, the user index is omitted in this section for notation simplicity.

### A. Sector Beampattern Selection

In this approach, a Rx dynamically selects $N_t$ beampatterns with the largest received powers out of all pre-designed directional beampatterns. Using the fast beamforming algorithms [10], [11], the set of reactance values, $\hat{\boldsymbol{x}}_{s,1}$ can be optimized to steer the beam a look direction (e.g., $0°$) and also maximize the antenna efficiency. Due to the symmetric antenna structure, circularly shifting elements of $\hat{\boldsymbol{x}}_{s,1}$ is able to rotate the beampattern to different angular directions. Consequently, an $(M+1)$-element ESPAR is able to form $M$ directional beampatterns (referred to as sector beampatterns), denoted by the set $\mathcal{B}_s = \{B_{s,1}, \cdots, B_{s,M}\}$. As $\hat{\boldsymbol{x}}_{s,m}, m = \{2, \cdots, M\}$ is a circular shift of $\hat{\boldsymbol{x}}_{s,1}$ and the antenna topology is symmetric, the resultant $Z_{in,s,m}$ remains constant for all $M$ sector beampatterns. A Rx selects $N_t$ beamaptterns out of the set $\mathcal{B}_s$ by examining the received powers over all sector beampatterns, i.e., $B_n^\star = arg\max_{B_{s,m} \in \bar{\mathcal{B}}_s} P_r(B_{s,m}), n = \{1, \cdots, N_t\}, m = \{1, \cdots, M\}$, where $\bar{\mathcal{B}}_s$ is the subset of $\mathcal{B}_s$ by removing the previously selected beampatterns (for $n = 1$, $\bar{\mathcal{B}}_s = \mathcal{B}_s$), and $P_r(B_{s,m})$ is the received power when $B_{s,m}$ is formed. In this approach, one extra symbol period is added in one super-symbol for beampattern selection. Therefore, the sum-rate in (6) is modified as

$$C' = \sum_{k=1}^{K} \frac{1}{N_t + K} \mathbb{E}\left\{\log\left|\boldsymbol{I}_{N_t} + \tilde{P}_t\tilde{\boldsymbol{H}}^{[k]}\tilde{\boldsymbol{H}}^{[k]H}\right|\right\}, \quad (7)$$

where $\tilde{P}_t = \frac{(N_t+K)P_t}{N_t(N_k+K-1)}$. Indeed, one extra symbol period used in one super-symbol leads to a reduction in DoF; however, the proposed method still works well for the low and moderate SNRs, due to directional beamforming.

### B. SVD Beamforming

An adaptive beamforming is proposed for the Rx ESPAR antenna, taking advantage of the available CSIR. Given the SVD beamforming, in a digital beamforming array using multiple RF chains, the weights for individual antenna elements can be independently obtained by digitally processing at baseband [12]; however, in the ESPAR array, the weights are tuned by adjusting reactance loads having a nonlinear relationship with the beampattern. The SVD beamforming with an Rx ESPAR antenna is proposed as a three-step design strategy, where a dynamic matching network is included to solve the problem of antenna efficiency.

*1) SVD Beamformer:* In the first step, the SVD beamformer aims to calculate weights based on the channel matrix estimated at the Rx. The reactance-domain (RD) technique, a common signal-processing technique for an ESPAR array [13], is employed to obtain a channel matrix analogous to that achievable in a digital beamforming array. In the RD technique, an ESPAR antenna forms $N_i (N_i \geq N_t)$ initial beampatterns, $\Phi_n(\theta), n = \{1, \cdots, N_i\}$, on a time division basis, where the same information signal is sent. In other words, during a block of $N_i$ sub-periods, the transmitted signal satisfies $\boldsymbol{s}(t_1) = \boldsymbol{s}(t_2) = \cdots = \boldsymbol{s}(t_{N_i})$. To simplify this method, antenna efficiency related to each of the initial beampatterns is assumed to be the same, i.e., $\eta_i = \eta, \forall i$, that can be achieved by simply using the sector beampatterns. According to (5), signals received over the initial beampatterns are represented as the $N_i$-dimensional vector:

$$\boldsymbol{y} = \sqrt{\eta}\left[\boldsymbol{h}^T(\Phi_1) \quad \cdots \quad \boldsymbol{h}^T(\Phi_{N_i})\right]\boldsymbol{s} + \boldsymbol{z} = \boldsymbol{H}_\Phi \boldsymbol{s} + \boldsymbol{z}, \quad (8)$$

where the $(i,j)$-th entry of the matrix $\boldsymbol{H}_\Phi \in \mathbb{C}^{N_i \times N_t}$ is the channel gain between the $i$-th initial beampattern and the $j$-th Tx antenna. The knowledge of $\boldsymbol{H}_\Phi$ is assumed to be available at the Rx. Perform SVD of $\boldsymbol{H}_\phi$, then one has

$$\boldsymbol{H}_\Phi = \boldsymbol{U}\boldsymbol{\Sigma}\boldsymbol{V}^H, \quad (9)$$

where $\boldsymbol{U} \in \mathbb{C}^{N_i \times N_i}$ and $\boldsymbol{V} \in \mathbb{C}^{N_t \times N_t}$ are unitary matrices, and $\boldsymbol{\Sigma} \in \mathbb{R}^{N_i \times N_t}$ is a diagonal matrix with $rank = \min(N_i, N_t) = N_t$ dominant singular values in a descending order as its diagonal entries. To provide $N_t$ beampatterns for BIA, the SVD beamformer applies the first $N_t$ column vectors of $\boldsymbol{U}$, denoted by $\boldsymbol{U}_{1:N_t}$, to the received signal in (10). The output of the SVD beamformer is

$$\boldsymbol{y}_{svd} = \boldsymbol{U}^H_{1:N_t}\boldsymbol{H}_\Phi \boldsymbol{s} + \boldsymbol{U}^H_{1:N_t}\boldsymbol{z}, \quad (10)$$

where the post-processed noises $\boldsymbol{U}^H_{1:N_t}\boldsymbol{z}$ are still AWGNs, since $\boldsymbol{U}$ is a unitary matrix.

*2) GA for Reactance Calculation:* In the second step, the GA is used to calculate $N_t$ sets of optimal reactance loads for beampatterns approximating to the output of the SVD beamformer. One of the most significant benefits of GA compared to other stochastic based ESPAR beamforming

algorithms [14] is that it avoids becoming stuck in the local minima and the requirement of gradient calculation.

The objective function of the GA is to optimize reactance loads for the maximization of the cross-correlation coefficient (CCC) between the achievable signal and the output of SVD beamformer. By maximizing the CCC, the designed beampatterns are able to approximate to the beampatterns defined by the SVD beamformer. The objective function is written as

$$\max_{\hat{\boldsymbol{x}}_n} \frac{\mathbb{E}\{y(\hat{\boldsymbol{x}}_n)\boldsymbol{y}^*_{svd}(n)\}}{\sqrt{\mathbb{E}\{y(\hat{\boldsymbol{x}}_n)y(\hat{\boldsymbol{x}}_n)^*\}\mathbb{E}\{\boldsymbol{y}_{svd}(n)\boldsymbol{y}^*_{svd}(n)\}}}, \quad (11)$$

where $y(\hat{\boldsymbol{x}}_n), n = 1, \cdots, N_t$, is the received signal when the set of reactance loads, $\hat{\boldsymbol{x}}_n$, is used.

Considering the binary-encoded GA, each of the optimization variable – a reactance load ($x_m$), is encoded into $N_g$ binary bits (e.g., $x_m$ = 101$\cdots$1) – which is referred to as a gene. The set of $M$ genes constitutes a chromosome with the length of $M \cdot N_g$ bits (e.g., *chromosome* = (101$\cdots$1)(001$\cdots$1)$\cdots$(110$\cdots$0)). The GA starts by randomly generating a large number ($N_{ch}$) of chromosomes, referred to as the first generation. Each chromosome is assigned a fitness value, which is the CCC given in (11). According to the fitness values, an appropriate portion of chromosomes is selected as "parents" by the roulette wheel selection method [15]. The selected chromosomes are paired to operate one-point crossover [15] to produce two offspring. Finally, mutation is performed in the produced offspring. In particular, the mutation is to randomly select a small percentage of bits from the produced chromosomes and then change the selected bits from "1s" to "0s" or vice versa. The above processes are repeated until convergence or until the pre-determined maximum number of generations is exceeded.

*3) Impedance Matching:* Generally, an ESPAR antenna is an unmatched system, where the active element is directly connected to the RF source with $Z_s$. Since the optimized reactance loads obtained by GA are based on SVD beamforming, which cannot guarantee the matching between $Z_{in,n}$ and $Z_s$, antenna efficiency is still an issue. Here, to minimize mismatching between $Z_s$ and $Z_{in,n}$, a dynamic matching network (DMN) [16] is added between the RF port and the ESPAR array to form a closed-loop control system. The dynamic matching circuits can be realized with the varactors; however, the circuit design is beyond the scope of this study. It is noted that, under perfect matching between $Z_{in,n}$ and $Z_s$ (thus, $\eta_n$ = 100%), the output impedance of the DMN, $Z_{out,n}$, is equal to the complex conjugate of the input impedance, i.e., $Z_{out,n} = Z^*_{in,n}$ [16]. Using the DMN, the loading matrix is modified as $\boldsymbol{X}_n = diag([Z_{out,n}, j\hat{\boldsymbol{x}}_n^T])$.

## IV. Simulation Results

In this section, we evaluate performance of the proposed beamforming methods. The achievable sum-rate of the BIA system is used as the metric, and the rate achieved in a SU-MISO BC is considered as the baseline for comparison. The rate of a SU-MISO BC is $C = \mathbb{E}\left\{log\left|\boldsymbol{I}_{N_t} + \frac{P_t}{N_t}\boldsymbol{h}_{omni}\mathbf{h}^H_{omni}\right|\right\}$, where $\mathbf{h}_{omni} \in \mathbb{C}^{1\times N_t}$ is the channel vector corresponding to an omni-directional beampattern formed by the Rx ESPAR antenna for fair comparison.

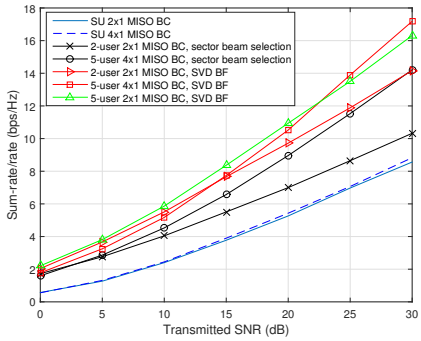


Fig. 2: Simulated results of ESPAR-based BIA with the sector beampattern selection and SVD-based beamforming, no CSI overheads considered.

The reactance loads for omni-directional beampattern are $\hat{\boldsymbol{x}} = [-259.06, -219.7, -268.43, 217.6, -260.82, -222.14]$ and $\eta$ = 84%. Moreover, the ESPAR-based BIA schemes are also compared to the CSIT-based linear zero-forcing beamforming (LZFBF). In this simulations, $N_s$ = 20 is assumed and the simulated results are averaged from 1000 Monte-Carlo experiments. The Tx is equipped with a uniform linear array with spacing of $\lambda/2$ ($\lambda$ is the wavelength). The simulated ESPAR antenna is composed of $M + 1 = 7$ thin electrical dipoles with length of $\lambda/2$, and the inter-element spacing is set to $\lambda/4$.

We first consider the performance of proposed beamforming methods without considering CSI overheads. The 6 sector beampatterns are formed by using and circularly shifting the optimized reactance values, $[-33.4, 160.7, 80.7, -160.1, -33.2, -71.9]$, with $\eta \approx 100\%$. To operate the SVD beamforming, the sector beampatterns given above are used as the initial beampatterns to achieve the channel matrix $\boldsymbol{H}_\Phi \in \mathbb{C}^{6\times N_t}$. The parameters for GA algorithm are: number of genes $M$ = 6, bits per gene $N_g$ = 12, reactance value limit of ±300Ω, population size $N_{ch}$ = 100, 500 generations, crossover probability of 0.7 and mutation probability of 0.1.

The simulated results are given in Fig. 2. With the sector beampattern selection, DoFs achieved by BIA fully describe the capacity, since sum-rate of the MU-MISO BC is much higher than that of the SU-MISO BC over all transmitted SNRs considered. It is also observed that sum-rate achieved by SVD beamforming is even higher than that achieved by sector beampattern selection at the expenses of computational complexity. However, with the SVD beamforming, the sum-rate with $K = 5, N = 4$ is inferior to that with $K = 2, N_t = 2$, when $SNR \leq 15$ dB. The reason is that the increase of $N_t$ requires more beampatterns designed by the SVD beamforming, and the SVD beamformer designs beampatterns exploiting the initial beampatterns. Thus, given a number of initial beampatterns, when $N_t$ is much smaller than $N_i$, a Rx benefits from the more flexible beamforming. When $N_t$ is approximate to $N_i$, the performance with SVD beamforming degrades. Using more initial beampatterns with the increase of $N_t$ will be a solution; however, it is not practical, since

CSI overheads and complexity are increased. Therefore, the SVD beamforming is more suitable for a system with a small $N_t$. With the SVD beamforming, the cross between the curves of the 5-user $4 \times 1$ MISO BC and the 5-user $2 \times 1$ MISO BC around 22 dB implies that when SNR is high enough the DoFs can completely describe sum-rate gain.

Indeed, the benefits of the BIA scheme come from the reduction of the CSIT overhead. Therefore, the comparison between the LZFBF [17] and the ESPAR-based BIA takes into account both the CSIT and CSIR overheads. We analyze the performance comparison using the CSI overhead costs discussed in [3]. Specifically, we consider two cases depending on the CSI overhead costs, referred to as "OHL" (a case of smaller resource cost for CSI inquiry) and "OHU" (a case of larger resource cost). The overhead costs for LZFBF is $N_t\rho_{csi} + K\rho_{fb}+K\eta_{cd}$ [1] under OHL, and $N_t\rho_{csi}+KN_t\rho_{fb}+K\rho_{cd}$ under OHU; for BIA with beampattern selection, $N_t\rho_{cd}$ (or ) under OHL, and $(N_t)^2\rho_{cd}$ under OHU, while for BIA with SVD beamforming, $N_tN_i\rho_{cd}$ under UHL and $(N_t)^2N_i\rho_{cd}$ under UHO. In this context, the net-rate of a given technique is sum-rate without CSI overheads times one minus overheads costs.

Fig. 3 (a) shows the simulated net-rates of the LZFBF and ESPAR-based BIA schemes for the 2-user $2 \times 1$ MU-MISO BC, with $\rho_{csi} = \rho_{cd} = 1\%$ and two distinct $\rho_{fb}$ values: $1\%$ and $3\%$. It is observed that, in the low transmitted SNR region, the BIA schemes with sector beampattern selection and SVD beamforming are superior to the LZFBF. Moreover, the figure reveals that, for the BIA schemes with sector beampattern selection, there is no significant difference between the rate performance in the OHL and OHU cases. Nevertheless, large rate loss is observed by the BIA scheme with SVD beamforming and LZFBF in the OHU case, emphasizing the importance of the CSI overhead designs in both of the two schemes. Fig. 3 (b) depicts simulated results for the 4-user $4 \times 1$ MU-MISO BC, which illustrates that the impact of the CSI overheads on the net-rates becomes more significant with the increase of $N_t$ and $K$. Take the BIA with SVD beamforming for example, its rate gains are totally lost in the OHU case, since it requires more resources for CSI acquisition (i.e., $N_i$ times more that the beam selection).

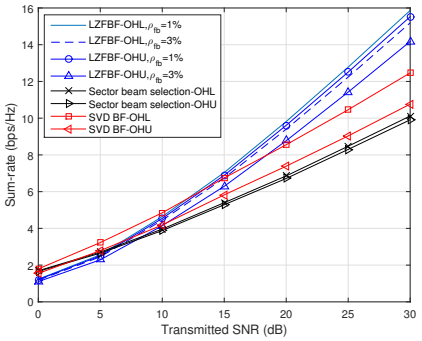


(a) 2-user $2 \times 1$ MISO BC

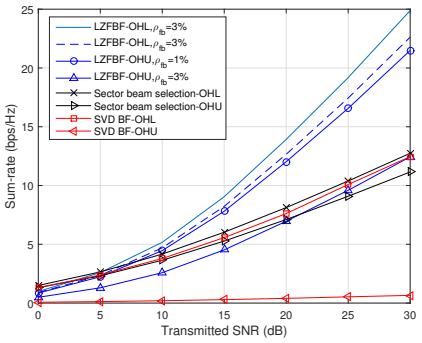


(b) 4-user $4 \times 1$ MISO BC

Fig. 3: Rate performance comparison between LZFBF and ESPAR-based BIA schemes taking CSI overheads into account.

## V. Conclusion

BIA is a promising technique for MU-MISO BC with no CSIT. In this work, the ESPAR antenna is considered as a practical solution for beampattern switching to implement the BIA scheme. To implement BIA, this work exploited the ESPAR antenna as the beampattern switching solution at the receiving end. Two ESPAR beamforming methods are proposed to improve the performance of BIA, where the antenna efficiency has been taken into account. Both of the sector beampattern selection and SVD beamforming show their capabilities to increase the sum-rate in the BIA system. Moreover, the CSI overheads are also considered in the simulations to illustrate the benefits of the proposed scheme.

[1] $\rho_{cis}$, $\rho_{cd}$ denote the fraction of the total downlink transmit resources used for estimation pilots per Tx antenna, and for coherent detection pilots per user, respectively, and $\rho_{fb}$ represents the fraction per user per Tx antenna of total downlink transmit resources used to support the uplink feedback [3].

## Acknowledgment

The authors would like to thank the EPSRC Project EP/M014126/1, Large Scale Antenna Systems Made Practical: Advanced Signal Processing for Compact Deployments [LSAS-SP] for funding.

## References

[1] T. Gou, C. Wang, and S. A. Jafar, "Aiming perfectly in the dark-Blind interference alignment through staggered antenna switching," *IEEE Trans. Signal Proc.*, vol. 59, no. 6, pp. 2734–2744, Jun. 2011.

[2] M. Sellathurai and S. Haykin, *Space-time layered information processing for wireless communications*. John Wiley & Sons, 2009, vol. 30.

[3] C. Wang, H. C. Papadopoulos, S. A. Ramprashad, and G. Caire, "Improved blind interference alignment in a cellular environment using power allocation and cell-based clusters," in *Proc. IEEE ICC*, 2011, pp. 1–6.

[4] ——, "Design and operation of blind interference alignment in cellular and cluster-based systems," in *IEEE Information Theory and Applications Workshop (ITA)*, 2011, pp. 1–10.

[5] T. Ohira and K. Gyoda, "Electronically steerable passive array radiator antennas for low-cost analog adaptive beamforming," in *Proc. IEEE International Conference on Phased Array Systems and Technology*, 2000, pp. 101–104.

[6] R. Qian, M. Sellathurai, and D. Wilcox, "On the design of blind interference alignment using ESPAR antenna," in *Proc. IEEE CHINACOM*, 2012, pp. 866–870.

[7] R. Qian and M. Sellathurai, "Performance of the blind interference alignment using espar antennas," in *Proc. IEEE ICC*, 2013, pp. 4885–4889.

[8] P. N. Vasileiou, K. Maliatsos, E. D. Thomatos, and A. G. Kanatas, "Reconfigurable orthonormal basis patterns using ESPAR antennas," *IEEE Antennas and Wireless Propag. Lett.*, vol. 12, pp. 448–451, Mar. 2013.

[9] T. Ohira, "Adaptive array antenna beamforming architectures as viewed by a microwave circuit designer," in *Proc. IEEE Asia – Pacific Microwave Conference*, 2000, pp. 828–833.

[10] D. Wilcox, E. Tsakalaki, A. Kortun, T. Ratnarajah, C. B. Papadias, and M. Sellathurai, "On spatial domain cognitive radio using single-radio parasitic antenna arrays," *IEEE J. Sel. Areas Commun.*, vol. 31, no. 3, pp. 571–580, Mar. 2013.

[11] R. Qian, M. Sellathurai, and D. Wilcox, "A study on MVDR beamforming applied to an ESPAR antenna," *IEEE Signal Process. Lett.*, vol. 22, no. 1, pp. 67–70, Jan. 2015.

[12] D. Wilcox and M. Sellathurai, "On MIMO radar subarrayed transmit beamforming," *IEEE Trans. Signal Process.*, vol. 60, no. 4, pp. 2076–2081, Dec. 2012.

[13] C. Plapous, J. Cheng, E. Taillefer, A. Hirata, and T. Ohira, "Reactance domain MUSIC algorithm for electronically steerable parasitic array radiator," *IEEE Trans. Antennas Propag.*, vol. 52, no. 12, pp. 3257–3264, Dec. 2004.

[14] C. Sun, A. Hirata, T. Ohira, and N. C. Karmakar, "Fast beamforming of electronically steerable parasitic array radiator antennas: Theory and experiment," *IEEE Trans. Antennas Propag.*, vol. 52, no. 7, pp. 1819–1832, Jul. 2004.

[15] M. Mitchell, *An introduction to genetic algorithms*. Cambridge, MA: MIT press, 1998.

[16] V Barousis and C Papadias, "Arbitrary precoding with single-fed parasitic arrays: Closed-form expressions and design guidelines," *IEEE Wireless Commun. Lett.*, vol. 3, pp. 229–232, Apr. 2014.

[17] T. Yoo and A. Goldsmith, "On the optimality of multiantenna broadcast scheduling using zero-forcing beamforming," *IEEE J. Sel. Areas Commun.*, vol. 24, no. 3, pp. 528–541, Mar. 2006.